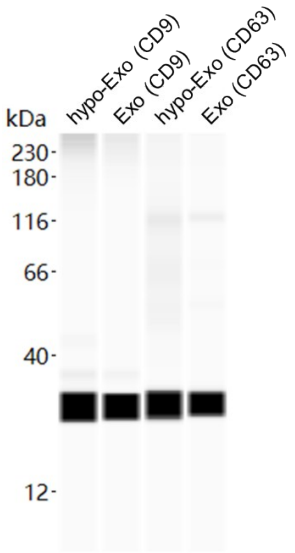

Fig. S1 Simple Western lane view of hypo-Exo and Exo tested with anti-CD9 and anti-CD63 primary antibodies.

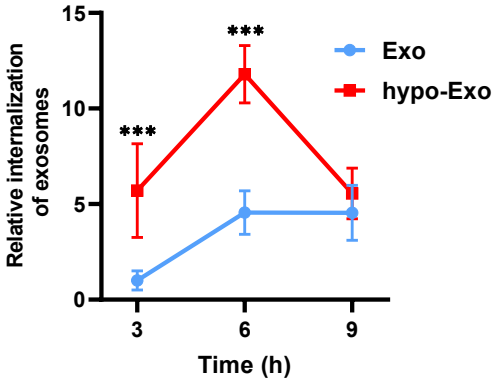

Fig. S2 Statistical analysis of intracellular exosomes fluorescence in HUVECs at various time (n=9).

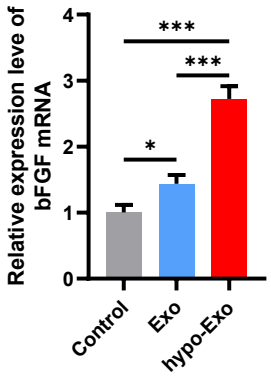

Fig. S3 Quantitative analysis of bFGF mRNA in HUVECs treated with PBS, Exo, and hypo-Exo (n=3).

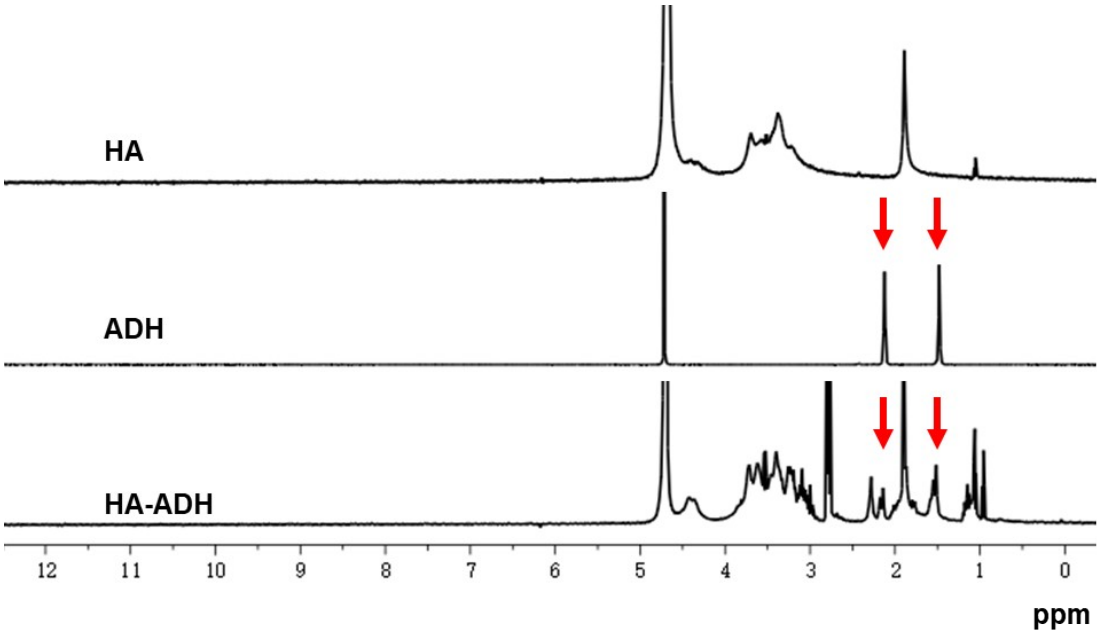

Fig. S4 ^{1}H NMR characterization of HA-ADH. Red arrows indicated related characteristic peaks of free ADH and HA-ADH.

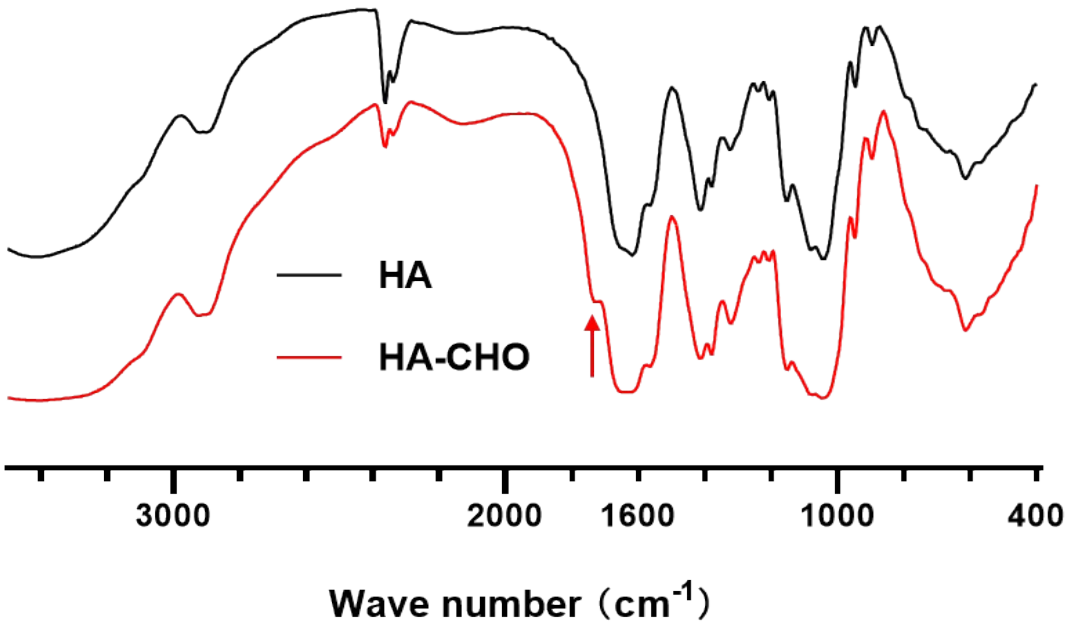

Fig. S5 FTIR characterization of HA-CHO. Red arrow indicated carbonyl absorption peak in the oxidized HA.

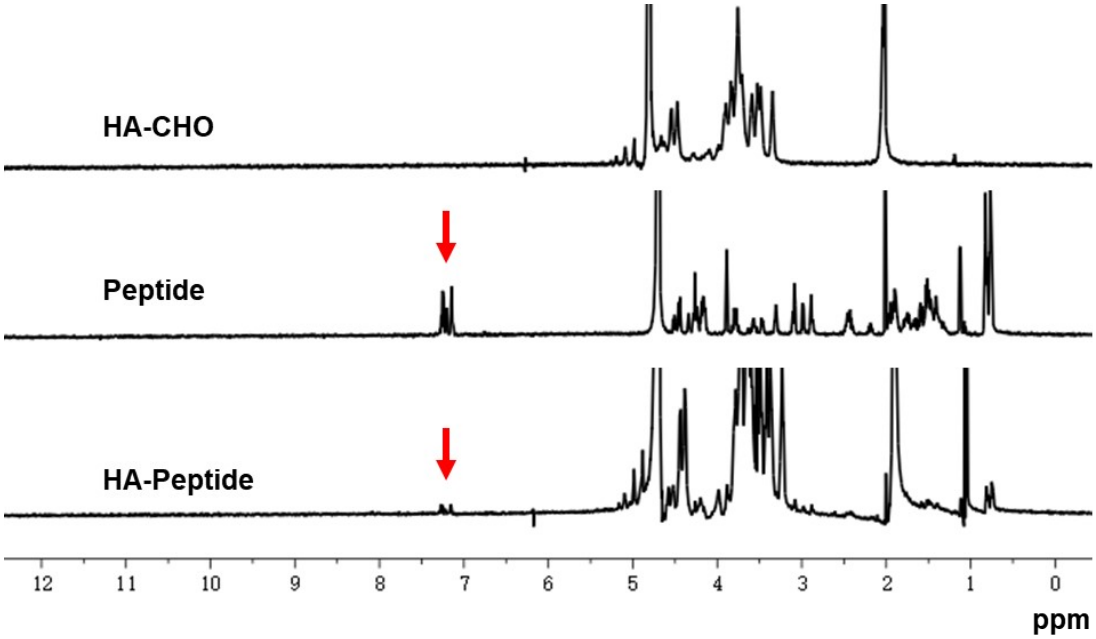

Fig. S6 ^{1}H NMR characterization of HA-Peptide. Red arrows indicated related characteristic peaks of free peptide and HA-Peptide.

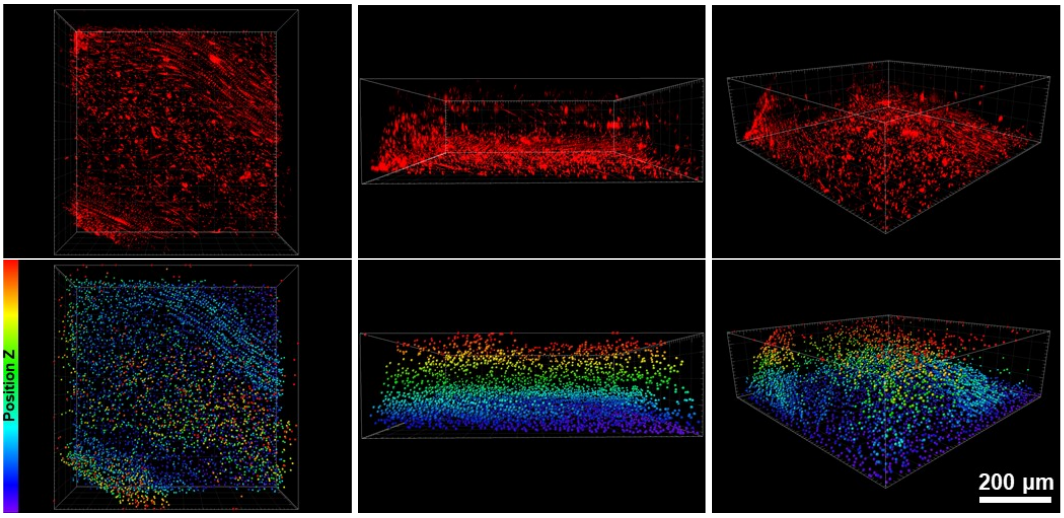

Fig. S7 Three-dimensional distribution of hypo-Exo in HA hydrogel. The hydrogel loading CM-DiI (red) labeled hypo-Exo was scanned with LSCM. The pseudo color remolding demonstrated the exosome spatial distribution according to position Z.

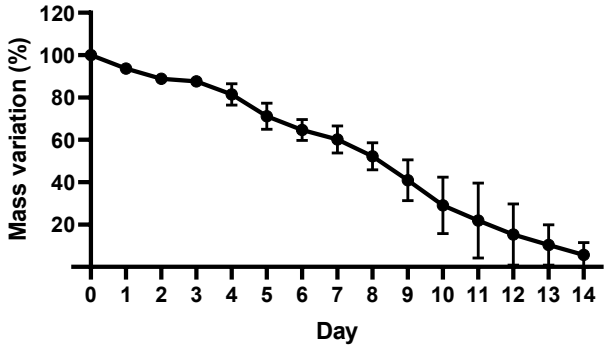

Fig. S8 Degradation of HA hydrogel in the culture medium.

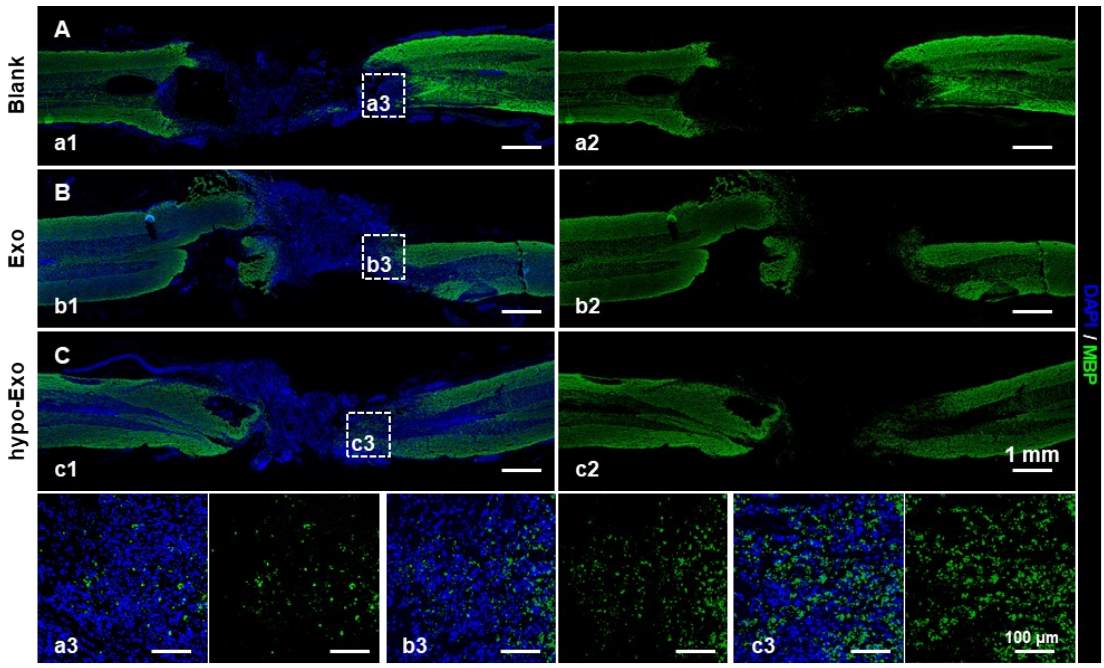

Fig. S9 Remyelination of injured spinal cord. The spinal immunofluorescence staining of myelin basic protein (MBP, green) in Blank (A), Exo (B), and hypo-Exo group (C) at 4-week post-surgery. The magnified views showed the detail of MBP distribution around the caudal stump (a3, b3, c3) boxed in (a1, b1, c1).

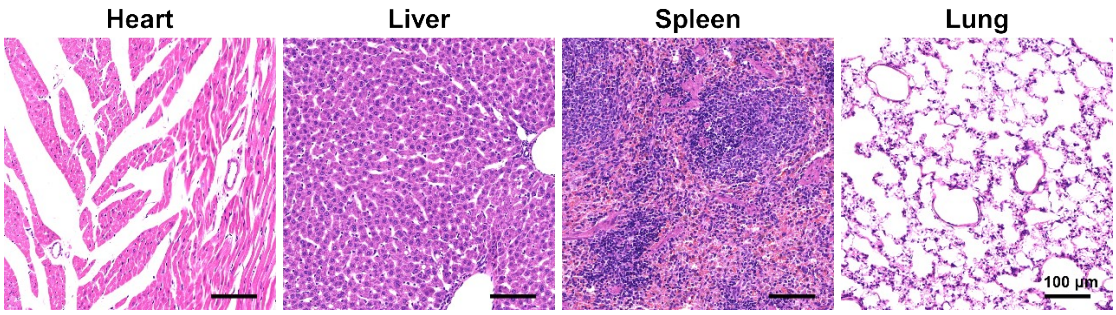

Fig. S10 HE staining of heart, liver, spleen, and lung in hypo-Exo group at 4-week post-surgery.